IEEE Access
Multidisciplinary ⋮ Rapid Review ⋮ Open Access Journal

Received 27 May 2024, accepted 29 July 2024, date of publication 9 August 2024, date of current version 19 August 2024.

*Digital Object Identifier 10.1109/ACCESS.2024.3441092*

RESEARCH ARTICLE

# Sliding Mode Without Reaching Phase Design for Automatic Load Frequency Control of Multi-Time Delays Power System

**DAO HUY TUAN[1], JAN PIDANIC[2], (Senior Member, IEEE), VAN VAN HUYNH[3], VO HOANG DUY[1], AND NGUYEN HUU KHANH NHAN[1]**

[1]Faculty of Electrical and Electronics Engineering, Ton Duc Thang University, Ho Chi Minh City 70000, Vietnam
[2]Department of Electronics and Radio Systems, Faculty of Electrical Engineering and Informatics, University of Pardubice, 532 10 Pardubice, Czech Republic
[3]Modeling Evolutionary Algorithms Simulation and Artificial Intelligence, Faculty of Electrical and Electronics Engineering, Ton Duc Thang University, Ho Chi Minh City 70000, Vietnam

Corresponding author: Van Van Huynh (huynhvanvan@tdtu.edu.vn)

**ABSTRACT** The automatic load frequency control (ALFC) is designed based on integral sliding mode control (ISMC) without reaching time for a multi-time delay power system (MTDPS) with the system disturbances and uncertainties. In contrast with a recent method, the time delay of an area control error (ACE) signal and an interconnected signal are deliberated for the ALFC design in the MTDPS. The sliding mode is proposed with a selection of an integral single-phase surface and control rules such that the sliding state variables begin at the surface at the initial moment and converge to zero without reaching time. In addition, Lyapunov-based new linear matrix inequality (LMI) is applied to analyze the entire power system's frequency steadiness. Moreover, the integral single-phase surface is advanced to improve the performance of the MTDPS. Using the proposed new integral single-phase surface approach, undershoot/overshoot and settling time were reduced compared to the recent (ISMC) approach. The results show the new scheme is highly robust in sliding variable's fast convergence to zero asymptotical compared to the recently designed SMC. It has no significant interruption in operation, making its application in real power systems possible.

**INDEX TERMS** Automatic load frequency control (ALFC), multi-area power system (MAPS), integral sliding mode control (ISMC), multi-time delay power system (MTDPS).

## I. INTRODUCTION

Automatic load frequency control (ALFC) has made a multi-time delay power system (MTDPS) reliable. Load frequency control (LFC) or automatic load frequency control plays the automatic generation control (AGC) role in maintaining the generation load balance by keeping power network area control error (ACE) stable. However, high frequency transient caused by various MTDPS problems such as higher order systems, a large number of state variables, nonlinearities, system parametric uncertainties, communication delays, random load disturbances, interconnection problems, etc., can undermine the efficacy of LFC for the MTDPS.

The associate editor coordinating the review of this manuscript and approving it for publication was Zheng Chen.

Over time, control engineers have developed different LFC schemes to stabilize the MTDPS under transient and various conditions. The common industrial one was the proportional-integral-derivative (PID) technique discussed in [1]. Another approach was decentralized LFC-based PID tuning to stabilize the interconnected power system (PS) given in [2]. The PID control scheme was also introduced to a stabilized PS with nonlinearities [3], [4]. Once more, the PID-based LFC has been applied for the PS with parametric uncertainties [5], [6]. In studies, the PID tuning to determine appropriate gain to stabilize PS transient is usually time-consuming and results in high overshoots if not properly tuned. Therefore, intelligent (fuzzy and neural network) control was established to improve PID tuning. Fuzzy logic is widely applied to tune the PID controller parameters [7]. Also, the fuzzy H-infinity

iterative learning approach for LFC of the PS has been discussed in [8]. In intelligent control design, fuzzy set decisions and neural network hidden layers should be accurate. However, these are difficult to formulate and applicable for the ALFC of the MTDPS.

Meanwhile, a superior technique combined with an intelligent control design based on the PID approach was developed. Various optimal schemes in combination with fuzzy and neural network based PID were applied to improve optimal searching and tuning for ALFC of the PS [9], [10], [11], [12], [13], [14], [15]. Optimal approaches combined with PID for ALFC of the PS were given in [16], [17], [18], [19], and [20]. The above traditional control methods can be put into operation in the ALFC of a small-scale system with nominal parameters. However, these methods cannot effectively handle complex ALFC problems in the MTDPS. To solve the above problem, variable structure control (VSC) based ALFCs are used nowadays for more complex power systems. The main mode of VSC is the sliding mode control (SMC). The SMC is applied to have the advantages of its insensitivity and robustness against numerous system problems, such as matched uncertainties and load disturbances. The SMC has been applied for the ACE solution of ALFC in the PS given in [21], [22], [23], and [24]. Adaptive approaches were combined with SMC to achieve good PS transient response [25], [26], [27], [28]. Also, some authors have applied an SMC based disturbance observer to stabilize the PS [21], [29], [30]. The SMC based state estimator for ALFC of the PS was given in [31] and [32]. However, the approaches above acted under the first order SMC, but the first-order SMC suffered from the chattering. This was due to neglected un-modelled dynamics, which caused harmonics and low control accuracies. Therefore, a higher-order SMC based ALFC was developed to solve the above problems. Chattering was eliminated in the SMC by using the second order given in [33]. An adaptive second-order SMC was applied to eliminate chattering caused by parametric uncertainties in the system state matrix discussed in [34]. The higher-order SMC based disturbance observer was introduced for ALFC of the PS [35]. The above approaches achieved the stability of ACE in the PS. However, during the PS operation, there is sometimes an ACE time delay in the closed-loop communication link. This is a result of communication delay. Therefore, the ALFC for the PS needs proper investigations under communication delay. However, the above higher order-SMC schemes are limited in practical application because of no time delay consideration. Fractional proportional-integral based ALFC was applied to stabilize the single area time delay power system (SATDPS) [36]. The SATDPS were similar to micro-grids [36] which had no interconnection system and interconnection signal delay. In [37], frequency control of micro-grid under power dynamic and communication uncertainty was advanced. In [38], the intelligent energy management method is applied for the voltage/frequency (V/F) control of micro-grids, regarding power uncertainties and communication delay. In [39], the energy management platform is used for controlling the V/F of micro-grids index in the presence of renewable energy sources and battery energy storage system. The V/F control is the main challenge in microgrid operation and control. As stated in [36], the SATDPS is simple, while the stability analysis of MTDPS is complex because of interconnection problem and time delay in the interconnection signal. In addition, with the development of PS, interconnection system and interconnection signal delay cannot be discounted and may reduce the PS performance. Different from the above approaches, the H-infinity scheme was used to study ALFC in the multi areas PS with communication delay given in [40], [41], and [42]. However, the PS uncertainty was not considered which may affect the PS performance. Recently, the SMC was used for ALFC of the PS with communication delay discussed in [43], [44], [45], [46], and [47]. In [43], the PI switching surface is selected for designing ALFC of two area PS without parameter uncertainty consideration. The ALFC of PS with parameter uncertainty consideration using PI switching surface can be seen in [44]. In [45] and [46], proportional switching function is designated for ALFC of PS with model matched and mismatched non-linear disturbances. In [47], the fractional-order PI sliding surface is developed for ALFC of the PS with load disturbance. The ALFC problems in PS with communication delay can be solved by the above methods via the SMC approach. However, two limitations were presented. First, the time delay in the interconnection signals was not considered [40], [41], [42] which may lead to PS instability. Second, the integral sliding surface in the approaches above depends on reaching time [43], [44], [45], [46], [47] which may degrade the PS performance. Therefore, these problems are solved with the proposed ISMC without reaching a time approach for the ALFC of MTDPS. The main benefits of the proposed ISMC without reaching time for the ALFC of MTDPS are presented below:

- The time delay of an ACE signal and an interconnected signal are considered for ALFC design in MTDPS which is a benefit for the modern PS with multi areas and interconnected systems.

- This is the first time the ISMC without reaching time is developed for ALFC of the MTDPS intending to improve the control performance.

- The MTDPS performance is improved because of system state trajectories in the sliding mode at the beginning time and avoiding undesirable switching law.

- Simulation results show better frequency deviation, better control performance in terms of short setting time, and a miniature overshoot compared to recent results.

## II. MATHEMATICAL MODEL OF MULTI-TIME DELAYS POWER SYSTEMS

A multi-time delay power system (MTDPS) is modeled in this partition. Figure 1 shows the block illustration of the $i^{th}$ area of the MTDPS. The $i^{th}$ area MTDPS model is based on a non-linear governor, a non-reheat steam chest turbine, and a generator rate constraint. The ALFC ensures tie-line power

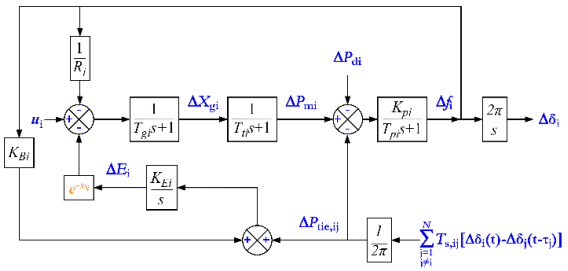


**FIGURE 1.** ALFC model of the i[th] area of the MTDPS.

fluctuation and frequency deviation within the limited ranges. Moreover, the multi time delay of ACE and interconnection signal are considered and denoted as $e^{-st}$.

$$\Delta\dot{f}_i(t) = -\frac{1}{T_{pi}}\Delta f_i(t) + \frac{K_{Pi}}{T_{pi}}\Delta P_{mi}(t) - \frac{K_{Pi}}{T_{pi}}\Delta P_{di}(t) - \frac{K_{Pi}}{2\pi T_{pi}}\sum_{j=1,j\neq i}^{N} T_{s,ij}[\Delta\delta_i(t) - \Delta\delta_j(t-\tau_j)] \quad (1)$$

$$\Delta\dot{P}_{mi}(t) = -\frac{1}{T_{ti}}\Delta P_{mi}(t) + \frac{1}{T_{ti}}\Delta X_{gi}(t) \quad (2)$$

$$\Delta\dot{X}_{gi}(t) = -\frac{1}{T_{gi}R_i}\Delta f_i(t) - \frac{1}{T_{gi}}\Delta X_{gi}(t) - \frac{1}{T_{gi}}\Delta E_i(t-\tau_i) + \frac{1}{T_{gi}}u_i(t) \quad (3)$$

$$\Delta\dot{E}_i(t) = K_{Bi}K_{Ei}\Delta f_i(t) + \frac{K_{Ei}}{2\pi}\sum_{j=1,j\neq i}^{N} T_{s,ij}[\Delta\delta_i(t) - \Delta\delta_j(t-\tau_j)] \quad (4)$$

$$\Delta\dot{\delta}_i(t) = 2\pi\ \Delta f_i(t) \quad (5)$$

where $i = 1$ to $N$, and $N$ are represented by the number of areas. $T_{s,ij}$ $(i \neq j)$ describes the coefficient of interconnected tie-line between $i^{th}$ area and $j^{th}$ area, $u_i$ means the control signal, $\Delta f_i(t)$ implies the frequency deviation of the area with $(i = 1,2\ldots)$, $\Delta P_{mi}(t)$ describes the mechanical power, $\Delta X_{gi}(t)$ denotes the position change of the governor valve, $\Delta\delta_i(t)$ and $\Delta\delta_j(t)$ mean the changes of rotor angle, $\Delta P_{di}(t)$ denotes the external load disturbances of each area, $T_{gi}$ shows time constant of the nonlinear governor, $T_{ti}$ describes the steam turbine time constant, $T_{pi}$ indicates time constant in the power network, $K_{Ei}$ describes speed regulation coefficient, $K_{pi}$ implies power network gain, $K_{Bi}$ indicates frequency bias factor and $R_i$ shows speed droop coefficient of area $i^{th}$.

- $\Delta E_i(t - \tau_i)$ represents area control error time delay. Next, to design the highly robust SMC without reaching time, we represent the dynamic relations of equations (1) to (5) in the state variable space form.

$$\dot{z}_i(t) = A_i z_i + A_{id_i} z_{id_i} + B_i u_i + \sum_{j=1;j\neq i}^{N} H_{ij} z_{jd_j} + F_i \Delta P_{di}(t) \quad (6)$$

where $z_i(t) = \left[\Delta f_i(t)\ \Delta P_{mi}(t)\ \Delta X_{gi}(t)\ \Delta E_i(t)\ \Delta\delta_i(t)\right]^T$ is the state variable, $u_i(t)$ is the control input, and $A_i, B_i, D_i, F_i, H_{ij}$ are the state space matrixes given in the following.

$$A_i = \begin{bmatrix} \frac{-1}{T_{Pi}} & \frac{K_{Pi}}{T_{Pi}} & 0 & 0 & -\frac{K_{Pi}}{2\pi T_{Pi}}\sum_{j=1,j\neq i}^{N} T_{s,ij} \\ 0 & -\frac{1}{T_{Ti}} & \frac{1}{T_{Ti}} & 0 & 0 \\ -\frac{1}{R_i T_{Gi}} & 0 & -\frac{1}{T_{Gi}} & 0 & 0 \\ K_{Bi}K_{Ei} & 0 & 0 & 0 & \frac{K_{Ei}}{2\pi}\sum_{j=1,j\neq i}^{N} T_{s,ij} \\ 2\pi & 0 & 0 & 0 & 0 \end{bmatrix}$$

$$B_i = \begin{bmatrix} 0 \\ 0 \\ \frac{1}{T_{Gi}} \\ 0 \\ 0 \end{bmatrix};\quad F_i = \begin{bmatrix} -\frac{K_{Pi}}{T_{Pi}} \\ 0 \\ 0 \\ 0 \\ 0 \end{bmatrix};$$

$$D_i = \begin{bmatrix} 0 & 0 & 0 & 0 & 0 \\ 0 & 0 & 0 & 0 & 0 \\ 0 & 0 & 0 & -\frac{1}{T_{Gi}} & 0 \\ 0 & 0 & 0 & 0 & 0 \\ 0 & 0 & 0 & 0 & 0 \end{bmatrix};$$

$$H_{ij} = \begin{bmatrix} 0 & 0 & 0 & 0 & -\frac{K_{Pi}}{2\pi T_{Pi}}\sum_{j=1,j\neq i}^{N} T_{s,ij} \\ 0 & 0 & 0 & 0 & 0 \\ 0 & 0 & 0 & 0 & 0 \\ 0 & 0 & 0 & 0 & \frac{K_{Ei}}{2\pi}\sum_{j=1,j\neq i}^{N} T_{s,ij} \\ 0 & 0 & 0 & 0 & 0 \end{bmatrix}$$

If we consider the uncertainty in the form of the position change of the governor valve, then the equation (6) is further rewritten as

$$\begin{aligned} &\dot{z}_i \\ &= [A_i + \Delta A_i(z_i,t)]z_i + [A_{id_i} + \Delta A_{id_i}(z_i, t-\tau_i)]z_{id_i} \\ &\quad + B_i u_i(t) + \sum_{j=1;j\neq i}^{N} [H_{ij} + \Delta H_{ij}(z_j, t-\tau_j)]z_{jd_j} + F_i \Delta P_{di}(t) \\ &= A_i z_i + A_{id_i} z_{id_i} + B_i u_i + \sum_{j=1;j\neq i}^{N} H_{ij} z_{jd_j} + w_i(z_i,t) \end{aligned} \quad (7)$$

where $A_i, A_{id_i}, B_i, H_{ij}$ represent the system matrices with nominal value, $\Delta A_i(z_i,t)$, $\Delta H_{ij}(z_j, t-\tau_j)$, $\Delta A_{id_i}(z_i, t-\tau_i)$ denote the parameter uncertainties and $w_i(z_i,t)$ shows the lumped uncertainty defined as

$$w_i(z_i,t) = \Delta A_i(z_i,t)z_i(t) + \Delta A_{id_i}(z_i, t-\tau_i)]z_{id_i} + \sum_{j=1;j\neq i}^{N} \Delta H_{ij}(z_j, t-\tau_j)]z_{jd_j} + F_i \Delta P_{di}(t) \quad (8)$$

Before we continue, some assumptions and lemmas are given during the design.

*Assumption 1:* The combine uncertainties $w_i(z_i, t)$ and the differential of $\dot{w}_i(z_i, t)$ are bounded so that $\|w_i(z_i, t)\| \leq \gamma_i$ and $\|\dot{w}_i(z_i, t)\| \leq \partial_i$, where $\|.\|$ is the matrix norm.

*Lemma 1 ([33]):* Let $\mathbf{Z}$ and $\mathbf{T}$ be actual matrices of the right size. Then, the matrix inequality achieves, for any scalar $\gamma > 0$,

$$\mathbf{Z}^T\mathbf{T} + \mathbf{T}^T\mathbf{Z} \leq \mu\mathbf{Z}^T\mathbf{Z} + \mu^{-1}\mathbf{T}^T\mathbf{T}.$$

*Lemma 2 ([48]):* If the matrix:

$$\begin{bmatrix} O(z) & \Pi(z) \\ \Pi^T(z) & \Xi(z) \end{bmatrix} > 0$$

then $\Xi(z) > 0$, and $O(z) - \Pi(z)\Xi^{-1}(z)\Pi^T(z) > 0$ where $O(z) = O^T(z)$, $\Xi(z) = \Xi^T(z)$, and $\Pi(z)$ are affinitively dependent on z.

*Remark 1:* The uncertainty consideration in this approach includes PS parameter uncertainty, load disturbance, the multi time delay of ACE and interconnection signal. This is a benefit for real applications of a complex modern PS.

## III. SLIDING MODE WITHOUT REACHING PHASE DESIGN

In practice, automatic load frequency control (ALFC) has the attractiveness of robustness against various forms of perturbation. In this regard, ALFC based integral sliding mode control (ISMC) without reaching time is designed. The ISMC design generally involves an arbitrary selection of sliding surfaces and control switching law. Here, we select a single-phase sliding surface so that sliding variables begin at the surface at a given moment and ensure the ISMC does not depend on reaching time. Thus, the integral single-phase surface is represented as:

$$\sigma_i[z_i(t)] = E_i z_i(t) - \int_0^t E_i(A_i - B_i T_i) z_i(\tau) d\tau - E_i z_i(0) e^{-\alpha_i t} \tag{9}$$

where $E_i$ is a constant matrix, and $E_i$ is constructed to warrant that $E_i B_i$ is an invertible matrix. $T_i$ is the design matrix, and matrix $T_i$ is preferred by polar assignment so that the eigenvalues of the matrix $(A_i - B_i T_i)$ are constantly negative. The term $E_i z_i(0) e^{-\alpha_i t}$ has been added which makes the ISMC without reaching time. Next, we design the control law. To begin, we differentiate the sliding surface $\sigma_i[z_i(t)]$ with respect to time hence, we arrive at the equation below.

$$\dot{\sigma}_i[z_i] = E_i[A_i z_i + A_{id_i} z_{id_i} + B_i u_i + \sum_{j=1; j\neq i}^{N} H_{ij} z_{jd_j} + w_i(z_i, t)] - E_i(A_i - B_i T_i) z_i + \alpha_i E_i z_i(0) e^{-\alpha_i t} \tag{10}$$

So, making $\sigma_i[z_i(t)] = \dot{\sigma}_i[z_i(t)] = 0$.

From the equation (10), $u_i^{eq}(t)$ is the equivalent control input, which is given as

$$u_i^{eq}(t) = -(E_i B_i)^{-1}[E_i A_i z_i + E_i A_{id_i} z_{id_i} + \sum_{j=1; j\neq i}^{N} E_i H_{ij} z_{jd_j} + E_i w_i(z_i, t) - E_i(A_i - B_i T_i) z_i(t) + \alpha_i E_i z_i(0) e^{-\alpha_i t}] \tag{11}$$

Before we design the control law, we investigate the MTDPS asymptotic stability in the sliding surface. To do that, we substitute the value of $u_i^{eq}$ into (7) and simplify as below:

$$\begin{aligned} \dot{z}_i &= (A_i - B_i T_i) z_i + [I - B_i(E_i B_i)^{-1} E_i] A_{id_i} z_{id_i} \\ &\quad + \sum_{j=1; j\neq i}^{N} [I - B_i(E_i B_i)^{-1} E_i] H_{ij} z_{jd_j} \\ &\quad + [I - B_i(E_i B_i)^{-1} E_i] w_i(z_i, t) \\ &\quad - B_i(E_i B_i)^{-1} E_i \alpha_i E_i z_i(0) e^{-\alpha_i t} \\ &= (A_i - B_i T_i) z_i + \Phi_i A_{id_i} z_{id_i} + \sum_{j=1; j\neq i}^{N} \Phi_i H_{ij} z_{jd_j} \\ &\quad + \Phi_i w_i(z_i, t) + \Theta_i z_i(0) e^{-\alpha_i t} \end{aligned} \tag{12}$$

where $\Phi_i = [I - B_i(E_i B_i)^{-1} E_i]$ and $\Theta_i = -B_i(E_i B_i)^{-1} E_i \alpha_i E_i$. Next, we examine the MTDPS stability theoretically. We start by representing the system state matrix as linear matrix inequality (LMI) accompanied by a basic theorem.

*Theorem 1:* The MTDPS (12) is asymptotically stable if and only if it embraces a symmetric positive matrix $Q_i$ $(i = 1, 2, .. .N)$, and positive scalars $q$, $\varphi_i$ and $\beta_j$ such that the next LMIs satisfy:

$$\begin{bmatrix} \Xi_i & A_{id_i}^T \Phi_i^T & Q_i \Phi_i Q_i \Theta_i \\ \Phi_i A_{id_i} & -\pi^{-1} \xi_i Q_i^{-1} & 00 \\ \Phi_i^T Q_i & 0 & -\chi_i 0 \\ \Theta_i^T Q_i 0 \; 0 & -\zeta_i & \end{bmatrix} < 0 \tag{13}$$

where

$$\Xi_i = [(A_i - B_i T_i)^T Q_i + Q_i(A_i - B_i T_i) + \kappa_i Q_i + \sum_{j=1; j\neq i}^{N} \hat{\pi} \beta_j H_{ji}^T \Phi_j^T Q_j \Phi_j H_{ji}].$$

Since the system with the LMI is a differential equation, to investigate the stability of the MTDPS (12), we apply the Lyapunov stability concept, where its function is given as

$$V = \sum_{i}^{N} z_i^T(t) Q_i z_i(t) \tag{14}$$

where $Q_i > 0$ satisfies (13). If we acquire the first-time derivative of (14) and simplify, we arrive at

$$\begin{aligned} \dot{V} &= \sum_{i=1}^{N} \{z_i^T(t)[(A_i - B_i T_i)^T Q_i + Q_i(A_i - B_i T_i)] z_i(t) \\ &\quad + z_{id_i}^T A_{id_i}^T \Phi_i^T Q_i z_i(t) + z_i^T(t) Q_i \Phi_i A_{id_i} z_{id_i} \\ &\quad + \sum_{j=1; j\neq i}^{N} z_{jd_j}^T H_{ij}^T \Phi_i^T Q_i z_i(t) + \sum_{j=1; j\neq i}^{N} z_i^T(t) Q_i \Phi_i H_{ij} z_{jd_j} \\ &\quad + w_i^T(z_i, t) \Phi_i^T Q_i z_i(t) + z_i^T(t) Q_i \Phi_i w_i(z_i, t) \\ &\quad + e^{-\alpha_i t} z_i^T(0) \Theta_i^T Q_i z_i(t) + z_i^T(t) Q_i \Theta_i z_i(0) e^{-\alpha_i t}\} \end{aligned} \tag{15}$$

When we apply Lemma 1 to the equation (15) and further simplify, we obtain

$$\begin{aligned}\dot{V} \le & \sum_{i=1}^{N}\{z_i^T(t)[(A_i-B_iT_i)^TQ_i+Q_i(A_i-B_iT_i)]z_i(t)\\ & +z_{id_i}^TA_{id_i}^T\Phi_i^TQ_iz_i(t)+z_i^T(t)Q_i\Phi_iA_{id_i}z_{id_i}\\ & +\sum_{j=1;j\neq i}^{N}z_{jd_j}^TH_{ij}^T\Phi_i^TQ_iz_i(t)+\sum_{j=1;j\neq i}^{N}z_i^T(t)Q_i\Phi_iH_{ij}z_{jd_j}\\ & +\chi_i^{-1}z_i^T(t)Q_i\Phi_i\Phi_i^TQ_iz_i(t)+\chi_iw_i^T(z_i,t)w_i(z_i,t)\\ & +\zeta_i^{-1}z_i^T(t)Q_i\Theta_i\Theta_i^TQ_iz_i(t)+\zeta_ie^{-\alpha_it}z_i^T(0)z_i(0)e^{-\alpha_it}\}\end{aligned} \tag{16}$$

If we also apply Lemma 1 to the equation (16) and simplify, we get

$$\begin{aligned}&\dot{V}\\ &\le\sum_{i=1}^{N}\{z_i^T(t)[(A_i-B_iT_i)^TQ_i+Q_i(A_i-B_iT_i)]z_i(t)\\ &+\xi_i^{-1}z_{id_i}^TA_{id_i}^T\Phi_i^TQ_i\Phi_iA_{id_i}z_{id_i}+\xi_iz_i^T(t)Q_iz_i(t)\\ &+\sum_{j=1;j\neq i}^{N}\beta_i^{-1}z_i^T(t)Q_iz_i(t)+\sum_{j=1;j\neq i}^{N}\beta_iz_{jd_j}^TH_{ij}^T\Phi_i^TQ_i\Phi_iH_{ij}z_{jd_j}\\ &+\chi_i^{-1}z_i^T(t)Q_i\Phi_i\Phi_i^TQ_iz_i(t)+\chi_iw_i^T(z_i,t)w_i(z_i,t)\\ &+\zeta_i^{-1}z_i^T(t)Q_i\Theta_i\Theta_i^TQ_iz_i(t)+\zeta_ie^{-\alpha_it}z_i^T(0)z_i(0)e^{-\alpha_it}\}\end{aligned} \tag{17}$$

Since

$$\begin{aligned}&\sum_{i=1}^{N}\sum_{j=1,j\neq i}^{N}\beta_iz_{jd_j}^TH_{ij}^T\Phi_i^TQ_i\Phi_iH_{ij}z_{jd_j}\\ &=\sum_{i=1}^{N}\sum_{j=1,j\neq i}^{N}\beta_jz_{id_i}^TH_{ji}^T\Phi_j^TQ_j\Phi_jH_{ji}z_{id_i},\end{aligned}$$

then we rewrite (17) in the following

$$\begin{aligned}\dot{V}\le & \sum_{i=1}^{N}\{z_i^T(t)[(A_i-B_iT_i)^TQ_i+Q_i(A_i-B_iT_i)]z_i(t)\\ & +\xi_i^{-1}z_{id_i}^TA_{id_i}^T\Phi_i^TQ_i\Phi_iA_{id_i}z_{id_i}\\ & +\xi_iz_i^T(t)Q_iz_i(t)+\sum_{j=1;j\neq i}^{N}\beta_i^{-1}z_i^T(t)Q_iz_i(t)\\ & +\sum_{j=1;j\neq i}^{N}\beta_jz_{id_i}^TH_{ji}^T\Phi_j^TQ_j\Phi_jH_{ji}z_{id_i}\\ & +\chi_i^{-1}z_i^T(t)Q_i\Phi_i\Phi_i^TQ_iz_i(t)+\chi_iw_i^T(z_i,t)w_i(z_i,t)\\ & +\zeta_i^{-1}z_i^T(t)Q_i\Theta_i\Theta_i^TQ_iz_i(t)+\zeta_ie^{-\alpha_it}z_i^T(0)z_i(0)e^{-\alpha_it}\}\end{aligned} \tag{18}$$

The matrix $A_{id_i}^T\Phi_i^TQ_i\Phi_iA_{id_i}$ is semi-positive definite.

Since the state variable are $z_i(t)$ for $i = 1, 2, \ldots, N$ independent of each other.

Then, the following is true

$$V(z_{1d_1}, z_{2d_2}, z_{3d_3}, \ldots, z_{nd_n}) \le \pi V(z_1, z_2, z_3, \ldots, z_n) \tag{19}$$

for $\pi > 1$, is corresponding to

$$\begin{aligned}&\sum_{i=1}^{N}\xi_i^{-1}z_{id_i}^TA_{id_i}^T\Phi_i^TQ_i\Phi_iA_{id_i}z_{id_i}\\ &\le\pi\sum_{i=1}^{N}\xi_i^{-1}z_i^TA_{id_i}^T\Phi_i^TQ_i\Phi_iA_{id_i}z_i\end{aligned} \tag{20}$$

which implies that

$$\begin{aligned}&\sum_{i=1}^{N}\sum_{\substack{j=1\\j\neq i}}^{N}\beta_jz_{id_i}^TH_{ji}^T\Phi_j^TQ_j\Phi_jH_{ji}z_{id_i}\\ &\le\hat{\pi}\sum_{i=1}^{N}\sum_{\substack{j=1\\j\neq i}}^{N}\beta_jz_i^TH_{ji}^T\Phi_j^TQ_j\Phi_jH_{ji}z_i\end{aligned} \tag{21}$$

where the scalar $\hat{\pi} > 1$ then, we can deduce the following inequality.

$$\begin{aligned}&\dot{V}\\ &\le\sum_{i=1}^{N}\{z_i^T(t)[(A_i-B_iT_i)^TQ_i+Q_i(A_i-B_iT_i)]z_i(t)\\ &+\pi\xi_i^{-1}z_i^TA_{id_i}^T\Phi_i^TQ_i\Phi_iA_{id_i}z_i+\xi_iz_i^T(t)Q_iz_i(t)\\ &+\sum_{j=1;j\neq i}^{N}\beta_i^{-1}z_i^T(t)Q_iz_i(t)+\sum_{j=1;j\neq i}^{N}\hat{\pi}\beta_jz_i^TH_{ji}^T\Phi_j^TQ_j\Phi_jH_{ji}z_i\\ &+\chi_i^{-1}z_i^T(t)Q_i\Phi_i\Phi_i^TQ_iz_i(t)+\chi_iw_i^T(z_i,t)w_i(z_i,t)\\ &+\zeta_i^{-1}z_i^T(t)Q_i\Theta_i\Theta_i^TQ_iz_i(t)+\zeta_ie^{-\alpha_it}z_i^T(0)z_i(0)e^{-\alpha_it}\}\end{aligned} \tag{22}$$

Based on Assumption 1, the next equation can be achieved

$$\begin{aligned}\dot{V}\le & \sum_{i=1}^{N}\{z_i^T(t)[(A_i-B_iT_i)^TQ_i+Q_i(A_i-B_iT_i)+\kappa_iQ_i\\ & +\chi_i^{-1}Q_i\Phi_i\Phi_i^TQ_i+\pi\xi_i^{-1}A_{id_i}^T\Phi_i^TQ_i\Phi_iA_{id_i}\\ & +\zeta_i^{-1}Q_i\Theta_i\Theta_i^TQ_i+\sum_{j=1;j\neq i}^{N}\hat{\pi}\beta_jH_{ji}^T\Phi_j^TQ_j\Phi_jH_{ji}]z_i(t)\\ & +\vartheta_i+\zeta_ie^{-\alpha_it}z_i^T(0)z_i(0)e^{-\alpha_it}\}\end{aligned} \tag{23}$$

where $\vartheta_i = \chi_i\gamma_i^2$ and $\kappa_i = \xi_i + \frac{N-1}{\beta_i}$.

From Lemma 2 and LMI (13), we get

$$\begin{aligned}\Lambda_i = & -[(A_i-B_iT_i)^TQ_i+Q_i(A_i-B_iT_i)+\kappa_iQ_i\\ & +\chi_i^{-1}Q_i\Phi_i\Phi_i^TQ_i+\pi\xi_i^{-1}A_{id_i}^T\Phi_i^TQ_i\Phi_iA_{id_i}\\ & +\zeta_i^{-1}Q_i\Theta_i\Theta_i^TQ_i+\sum_{j=1;j\neq i}^{N}\hat{\pi}\beta_jH_{ji}^T\Phi_j^TQ_j\Phi_jH_{ji}]>0\end{aligned} \tag{24}$$

Based on equations (23) and (24), we can infer

$$\dot{V}[z_i(t)] \leq \sum_{i=1}^{N} [-\lambda_{\min}(\Lambda_i) \|z_i(t)\|^2 + \upsilon_i + \zeta_i e^{-\alpha_i t} z_i^T(0) z_i(0) e^{-\alpha_i t}] \quad (25)$$

where $\upsilon_i$ is the constant value and $\lambda_{\min}(\Lambda_i) > 0$. The term $\zeta_i e^{-\alpha_i t} z_i^T(0) z_i(0) e^{-\alpha_i t}$ in equation (25) will converge to zero as the time approaches infinity. So, $\dot{V} < 0$ is achieved with $\|z_i(t)\| > \sqrt{\frac{\upsilon_i}{\lambda_{\min}(\Lambda_i)}}$.

Consequently, the MTDPS (12) is asymptotically stable.

*Remark 2: In the traditional SMC method, there are two phases which are the reaching phase and sliding phase. First, in the reaching phase, the switching control law is used to force the MTDPS variables into the sliding surface* $\sigma_i[z_i(t)] = \dot{\sigma}_i[z_i(t)] = 0$ *and remain on it thereafter. Second, the MTDPS in the sliding mode dynamic has good performance with the selection of the sliding surface. The integral sliding surface* $\sigma_i[z_i(t)] = E_i z_i(t) - \int_0^t E_i(A_i - B_i T_i) z_i(\tau) d\tau$ *can be seen in [43], [44], [45], [46], and [47]. The sliding surface is not equal to zero at the beginning time so, it takes time to derive the MTDPS variables into the sliding surface* $\sigma_i[z_i(t)] = \dot{\sigma}_i[z_i(t)] = 0$ *. However, the proposed integral single-phase surface given in equation (9) is equal to zero at the beginning time so that all the system state variable of MTDPS is in the sliding mode dynamic* $\sigma_i[z_i(t)] = \dot{\sigma}_i[z_i(t)] = 0$ *for all time which improves the control performance.*

## IV. DECENTRALIZED SLIDING MODE WITHOUT REACHING PHASE AUTOMATIC LOAD FREQUENCY CONTROL DESIGN

Automatic load frequency control (ALFC) for local control areas of the MTDPS is usually done using two control approaches: centralized and decentralized. Decentralized is widely used due to its advantage i.e., each local area can be controlled separately, and disturbance in one area will be handled without affecting other areas. Therefore, the decentralized sliding mode control using (9) and control law is developed as

$$\begin{aligned} u_i(t) &= -(E_i B_i)^{-1} [\|E_i\| \left\|A_{id_i}\right\| \left\|z_{id_i}\right\| + \sum_{j=1;j\neq i}^{N} \left\|E_j\right\| \left\|H_{ji}\right\| \left|z_{id_i}\right| \\ &\quad + \|E_i\| \gamma_i + \|E_i\| \|B_i\| \|T_i\| \|z_i\| \\ &\quad + \alpha_i \|E_i\| \|z_i(0)\| e^{-\alpha_i t} + \bar{\varepsilon}_i] \frac{\sigma_i[z_i(t)]}{\|\sigma_i[z_i(t)]\|} \end{aligned} \quad (26)$$

The control law (26) ensures that all the state variables are held in the all-time integral single phase sliding surface. To justify this statement, we again theoretically analyze the reachability of the sliding variables. We lay down a basic theorem.

*Theorem 2:* We consider MTDPS (7) with the decentralized ISMC in (26). Then, all solution orbits of the system state are kept in the all-time integral single phase sliding surface.

We again apply Lyapunov theory, where the function becomes

$$\bar{V}(t) = \sum_{i=1}^{N} \|\sigma_i[z_i(t)]\| \quad (27)$$

Thus, by differentiating the equation $\bar{V}(t)$ and simplifying then, we arrive at

$$\begin{aligned} &\dot{\bar{V}} \\ &= \sum_{i=1}^{N} [\frac{\sigma_i^T[z_i(t)]}{\|\sigma_i[z_i(t)]\|} \dot{\sigma}_i[z_i(t)]] = \sum_{i=1}^{N} \frac{\sigma_i^T[z_i(t)]}{\|\sigma_i[z_i(t)]\|} \\ &\quad \times \{E_i[A_i z_i + A_{id_i} z_{id_i} + B_i u_i + \sum_{j=1;j\neq i}^{N} H_{ij} z_{jd_j} \\ &\quad + w_i(z_i, t)] - E_i(A_i - B_i T_i) z_i + \alpha_i E_i z_i(0) e^{-\alpha_i t}\} \\ &= \sum_{i=1}^{N} \frac{\sigma_i^T[z_i(t)]}{\|\sigma_i[z_i(t)]\|} \{E_i A_{id_i} z_{id_i} + E_i B_i u_i + \sum_{j=1;j\neq i}^{N} E_i H_{ij} z_{jd_j} \\ &\quad + E_i w_i(z_i, t) + E_i B_i T_i z_i + \alpha_i E_i z_i(0) e^{-\alpha_i t}\} \end{aligned} \quad (28)$$

From the equation (28) and inequality properties $\|AB\| \leq \|A\| \|B\|$, one can infer

$$\begin{aligned} \dot{\bar{V}} &\leq \sum_{i=1}^{N} [\|E_i\| \left\|A_{id_i}\right\| \left\|z_{id_i}\right\| + \sum_{j=1;j\neq i}^{N} \|E_i\| \left\|H_{ij}\right\| \left|z_{jd_j}\right| \\ &\quad + \|E_i\| \|w_i(z_i, t)\| + \|E_i\| \|B_i\| \|T_i\| \|z_i\| \\ &\quad + \alpha_i \|E_i\| \|z_i(0)\| e^{-\alpha_i t}] + \sum_{i=1}^{N} \frac{G_i^T[z_i(t)]}{\|G_i[z_i(t)]\|} E_i B_i u_i(t) \end{aligned} \quad (29)$$

Using Assumption 1 we achieve

$$\begin{aligned} \dot{\bar{V}} &\leq \sum_{i=1}^{N} [\|E_i\| \left\|A_{id_i}\right\| \left\|z_{id_i}\right\| + \sum_{j=1;j\neq i}^{N} \left\|E_j\right\| \left\|H_{ji}\right\| \left|z_{id_i}\right| \\ &\quad + \|E_i\| \gamma_i + \|E_i\| \|B_i\| \|T_i\| \|z_i\| \\ &\quad + \alpha_i \|E_i\| \|z_i(0)\| e^{-\alpha_i t}] + \sum_{i=1}^{N} \frac{\sigma_i^T[z_i(t)]}{\|\sigma_i[z_i(t)]\|} E_i B_i u_i(t) \end{aligned} \quad (30)$$

Substituting the proposed control approach (26) into equation (30)

$$\dot{\bar{V}} \leq \sum_{i=1}^{N} -\bar{\varepsilon}_i \quad (31)$$

The above inequality conditions can infer that the system state trajectories of the MTDPS (7) is in the single phase sliding mode at the early time and remain in that mode afterward.

*Remark 3: The term* $E_i z_i(0) e^{-\alpha_i t}$ *which is a function of time indicates that the sliding variable's reachability to the surface does not depend on reaching time making it highly*

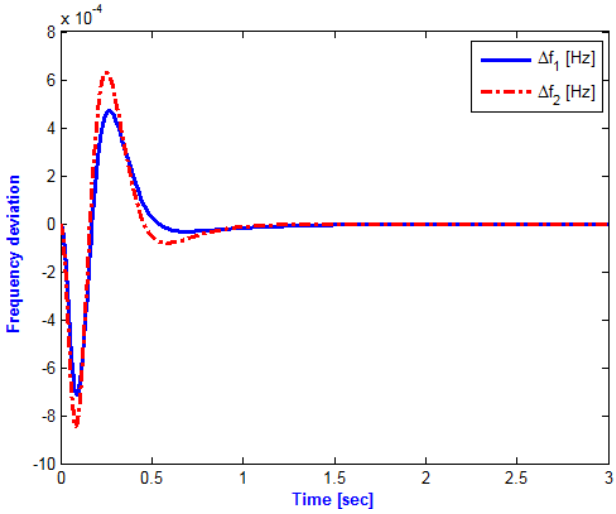


**FIGURE 2.** The system's frequency deviation in Hertz.

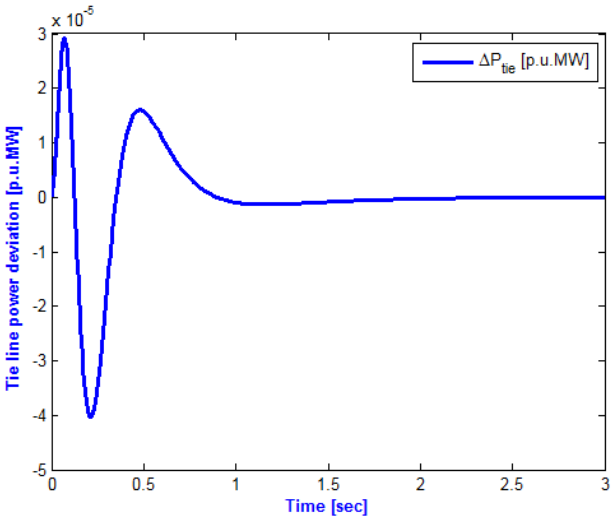


**FIGURE 3.** Variation inTLP.

*robust in contradiction of other SMCs discussed in the literature.*

*Remark 4: The multi time delay may reduce the performance of power systems or even worse lead to power system instability. In contrast with the methods given in [44], [45], [46], and [47], both the time delay of interconnection variable and the time delay of the ACE signal are considered in the proposed new ISMC without reaching time. This proved that the proposed method can be applied for the more general structure of the real MTDPS.*

## V. RESULTS AND DISCUSSIONS

This section, the proposed ISMC without reaching time is applied for ALFC of a two areas multi time delay power system (TAMTDPS). Four cases are given that examine enhanced ALFC of the TAMTDPS under load change, uncertainty, and parameter variation, and multi time delay. The TAMTDPS parameters and bounded conditions used for all four cases are shown in Tables 1 and 2 as given in [44]. All simulations are conducted in MATLAB® 8.3 (R2014a) on a Laptop Dell, 2.20 GHz (2 CPUs) Intel® Core(TM)2 Duo CPU T6670, 4096 MB RAM and Windows©7 Home Premium, 32-bit professional operating system.

**Case 1:** In case 1, the step load disturbances are provided as $\Delta P_{d1} = 0.01$, and $\Delta P_{d2} = 0.02$(p.u.MW). The multi time delay is programmed for the ACE signal of the two areas as $\tau_1 = 3.8$ (s) and $\tau_2 = 3.8$ (s) and the interconnected signal as $\tau_1 = 3.8$ (s) and $\tau_2 = 3.8$ (s), following the same instructions as [44], and the nominal TAMTDPS parameters are used. Figure 2 displays the TAMTDPS 's frequency deviations (FDs) in Hertz, and Figure 3 shows the TAMTDPS 's tie-line power (TLP) per unit. In Figure 4, the TAMTDPS's control signal is also perceptible. The frequency overshoot deviation (FOD) of area 1 and area 2 in Figure 2 are 0.00043 and 0.00062 in (Hz), respectively, which is a lesser value than the one reported in [44].

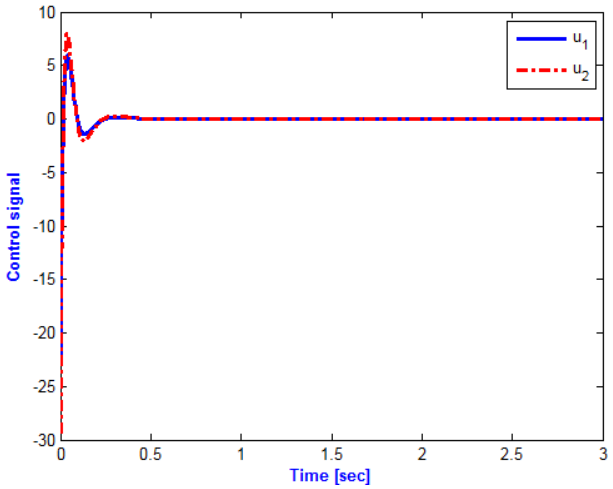


**FIGURE 4.** Control signal.

*Remark 5: Based on the maximum frequency overshoots (MFO), the proposed ISMC without reaching time is better in improving the ALFC of the TAMTDPS.*

**Case 2:** The TAMTDPS parameters and load conditions are the same as case 1. The multi time delay is configured the same for the ACE signal of the two areas, as $\tau_1 = 5$ (s) and $\tau_2 = 5$ (s), and the interconnected signal as $\tau_1 = 5$ (s) and $\tau_2 = 5$ (s). The mismatches parameter is provided in the system state matrix and the interconnection matrix as following $\Delta A_1$, as shown at the bottom of the next page, and $\Delta A_2 = \Delta A_3 = \Delta A_1$.

The mismatch between the subsystems is proposed below.

$$\Delta H_{12} = \begin{bmatrix} 0 & 0 & 0 & 0 & 0.2cos(t) \\ 0 & 0 & 0 & 0 & 0 \\ 0 & 0 & 0 & 0 & 0 \\ 0 & 0 & 0 & 0 & -0.3\sin(t) \\ 0 & 0 & 0 & 0 & 0 \end{bmatrix}$$

**TABLE 1.** Parameters of TAMTDPS.

| $T_{Pi}$ | $K_{Pi}$ | $T_{Ti}$ | $T_{Gi}$ | $R_i$ | $K_E$ | $\beta_i$ | $T_{Ii}$ |
|---|---|---|---|---|---|---|---|
| 10 | 1.0 | 0.3 | 0.1 | 0.05 | 0.4 | 21 | 0.1986 |

**TABLE 2.** Various bounded conditions.

| | $(1/K_{Pi})$ | $(K_{Pi}/T_{Pi})$ | $(1/T_{Ti})$ | $(1/T_{Gi})$ | $(1/R_i)$ |
|---|---|---|---|---|---|
| Nominal condition | 0.1 | 0.1 | 3.33 | 10 | 20 |
| Lower bound condition | 0.08 | 0.08 | 2.78 | 8 | 16.67 |
| Upper bound condition | 0.12 | 0.12 | 4.16 | 13.3 | 26 |

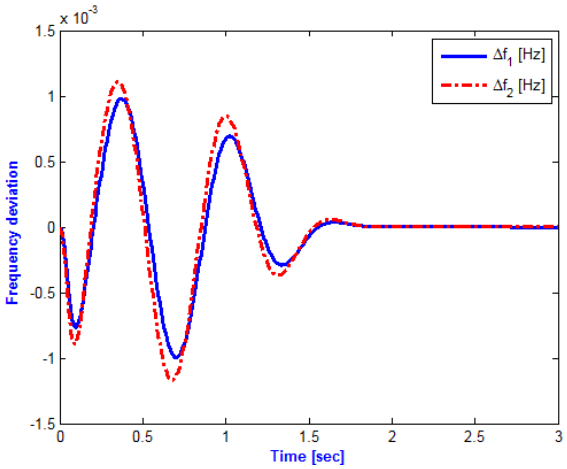


**FIGURE 5.** The system's frequency deviation in Hertz under mismatched uncertainty.

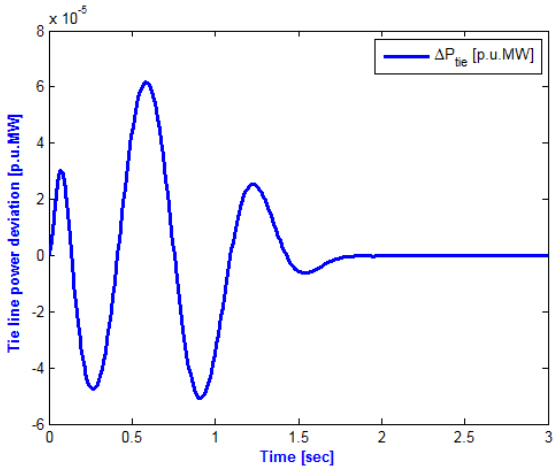


**FIGURE 6.** The TLP under mismatched uncertainty.

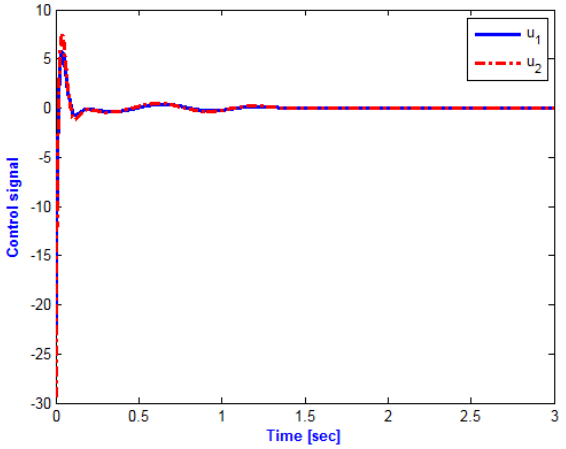


**FIGURE 7.** The system's control signal when the uncertainty is mismatched.

and $\Delta H_{12} = \Delta H_{23} = \Delta H_{31}$.

In Figure 5 and Figure 6, with the application of the proposed ALFC based ISMC without reaching time, the responses of FDs and the TLP come to a steady state after small fluctuations, and the output signals of control scheme in Figure 7 are close to usual operation state. In Figure 5, the FOA is maintained at $\pm 0.0011$Hz and damped to zero at 1.8s, which denotes that the new approach performs better than the one in [44].

*Remark 6: Both Figure 5 and Figure 6 indicate that the new approach is more robust in handling ALFC problems in MTDPS.*

**Case 3:** In this case, the various load disturbances are presented in Figure 8, and the nominal system parameters are varied to their lower bound, as indicated in Table 1. The multi time delay is selected for the ACE signal of the two areas as $\tau_1 = 3 - 0.5\sin(t)$(s) and $\tau_2 = 4 + 0.5\cos(t)$(s) and the interconnected signal as $\tau_1 = 3 - 0.5\sin(t)$(s) and $\tau_2 = 4 + 0.5\cos(t)$(s).

$$\Delta A_1 = \begin{bmatrix} 0 & 0.15\Delta f_1 & 0 & 0 & 0 \\ 0.15\sin(t) & 0 & 0 & 0 & 0 \\ 0 & 0 & 0.15\cos(t) & 0.15\cos(t) & 0 \\ 0 & 0 & 0 & 0 & 0.15\cos(t) \\ 0.15\cos(t) & 0 & 0 & 0 & 0 \end{bmatrix}$$

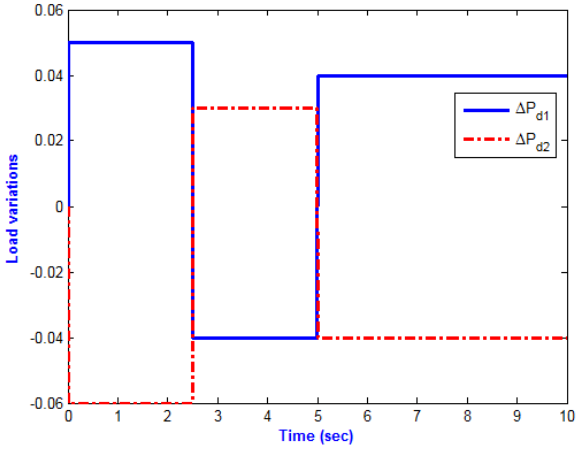


**FIGURE 8.** Load variations.

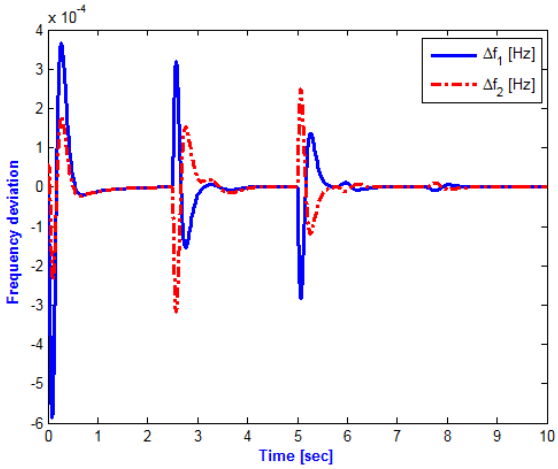


**FIGURE 9.** Frequency deviation.

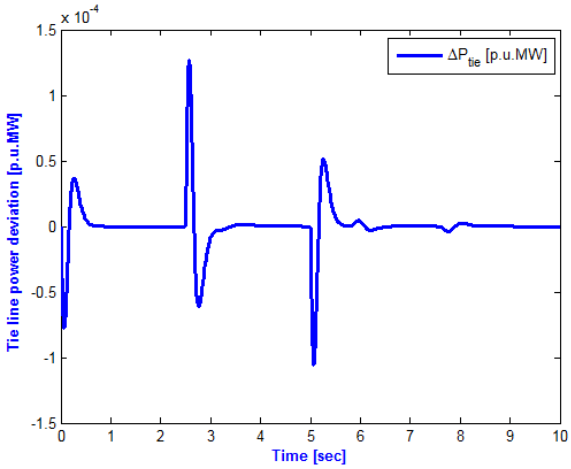


**FIGURE 10.** Deviation in tie-line power.

The results of the FD and the TLP, and control input are shown in Figures 9, 10, and 11 respectively.

*Remark 7: The TAMTDPS is considered under the multi time delay, parameter uncertainty, random load disturbance.*

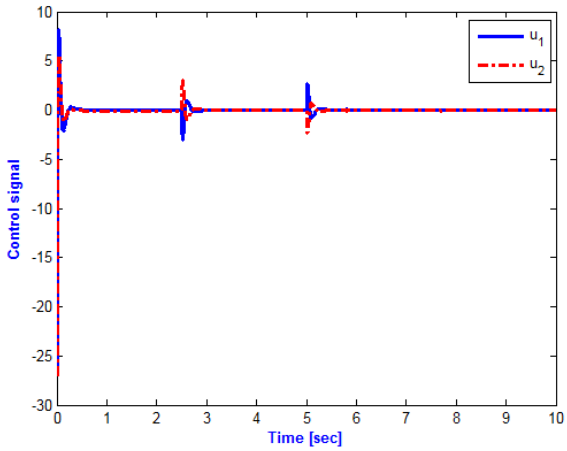


**FIGURE 11.** Signal of control.

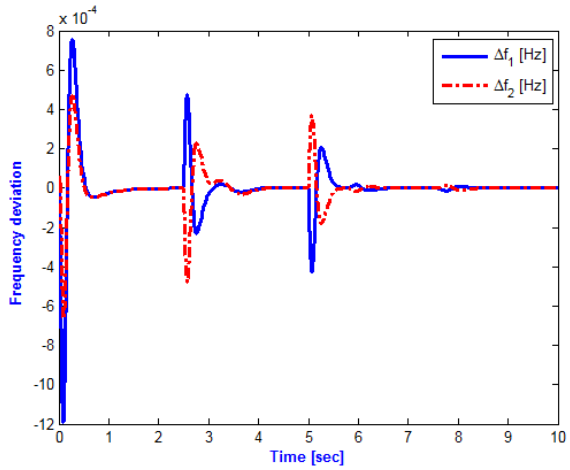


**FIGURE 12.** Frequency deviation.

*Figure 9 and Figure 10 prove the new scheme is highly robust and better performance in comparison with [44].*

**Case 4:** In this case, the simulation load conditions are the same as case 3 with the upper bound parameter of TAMTDPS.

The dynamic responses of the FD, the TLP, and controller of the TAMTDPS are illustrated in Figure 12, Figure 13, and Figure 14 respectively. Compared with the LFC based integral sliding mode control (ISMC) scheme with reaching time [44], the proposed ALFC based ISMC without reaching time scheme can actively compensate the perturbation caused by multi time delay, parameter uncertainty in the state and interconnection matrix, and load disturbance to ensure the resilient and continuous operation of power system.

*Remark 8: In the proposed ALFC based ISMC without reaching time scheme, the FD, the TLP responses quickly converge to stable state small steady-state control errors, which shows the proposed ALFC based ISMC without reaching time scheme can handle ALFC problems for the MTDPS more effectively than other methods discussed in the literature.*

**Case 5:** To show the effectiveness of the proposed method in comparison with different control methodologies, the proposed ALFC based integral single-phase sliding mode

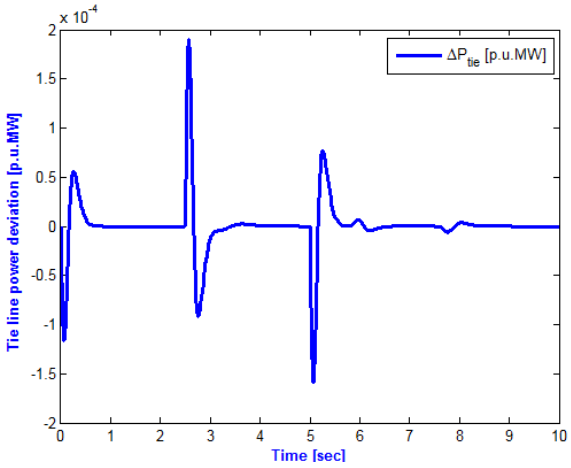


**FIGURE 13.** Deviation in tie-line power.

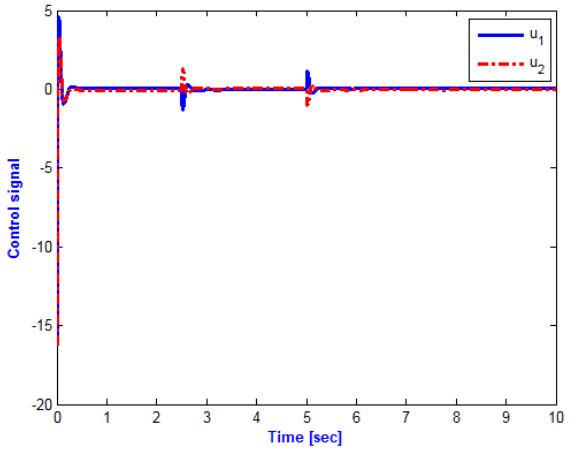


**FIGURE 14.** Signal of control.

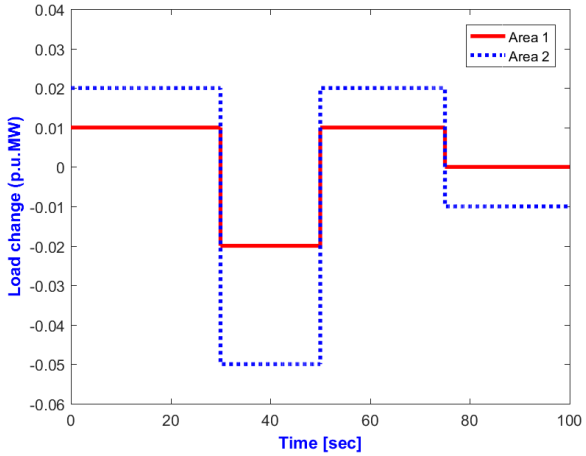


**FIGURE 15.** Load variation.

control (ISPSMC) without reaching time scheme is applied for MTDPS given in [47]. All the MTDPS parameters are the same with [47]. The multi time delay is selected for the ACE signal of the two areas as $\tau_1 = 3 - 0.5\sin(t)(\text{s})$ and $\tau_2 = 4 + 0.5\cos(t)(\text{s})$ and the interconnected signal as $\tau_1 = 3 - 0.5\sin(t)(\text{s})$ and $\tau_2 = 4 + 0.5\cos(t)(\text{s})$. The load variation and the FD are in Figure 15, Figure 16, and Figure 17, respectively. From Figure 16 and Figure 17, it can be observed that using the proposed ALFC based ISPSMC without reaching time scheme for MTDPS, a smaller frequency overshoot than the PID and ISMC approaches has been acquired.

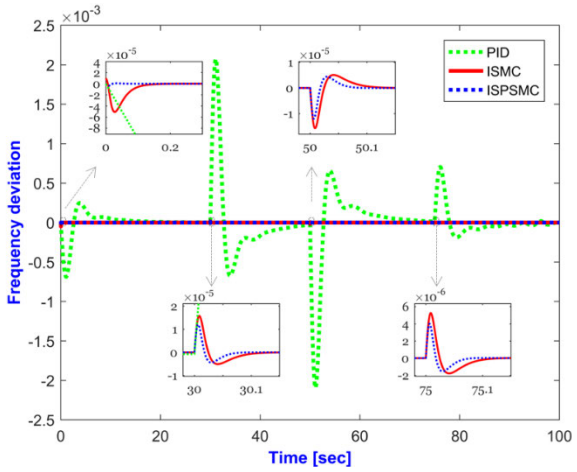


**FIGURE 16.** Frequency deviation of the area 1.

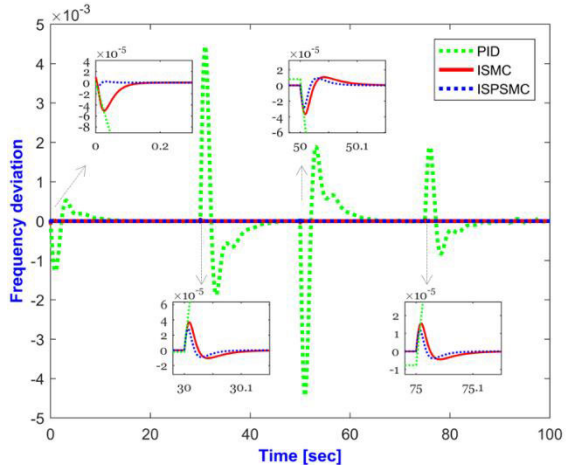


**FIGURE 17.** Frequency deviation of the area 2.

The above simulations display that the proposed ALFC based ISPSMC without reaching time scheme can not only decrease the influence of load disturbances on the MTDPS, but also guarantee fast response, smaller overshoot, and stronger robustness of the MTDPS.

## VI. CONCLUSION

In this paper, a decentralized ISMC without reaching time approach has been proposed to stabilize the power system with ACE time delay and interconnected time delay under the ALFC scheme. Compared with the recent SMC based AFLC, the proposed method is able to reduce the influence of multi time delay, parameter uncertainty, and load disturbance. Additionally, the MTDPS response has improved throughout the simulation in terms of minor overshoots and quick settling

times. This demonstrates that the new approach has strong viability in the application. Hence, it can be concluded that the proposed ISMC based ALFC scheme is not only robust in the presence of mismatched uncertainties and load disturbances, but also can be successfully applied to the multi time delay power system which will be beneficial to the electricity market. Despite the multi-time delay, the cyber-attacks may significantly influence the accuracy of the control system, which drives us to investigate this topic in the future.

## REFERENCES

[1] S. Saxena and Y. V. Hote, "Decentralized PID load frequency control for perturbed multi-area power systems," *Int. J. Electr. Power Energy Syst.*, vol. 81, pp. 405–415, Oct. 2016.

[2] M. Barakat, "Novel chaos game optimization tuned-fractional-order PID fractional-order PI controller for load–frequency control of interconnected power systems," *Protection Control Modern Power Syst.*, vol. 7, no. 1, pp. 1–20, Dec. 2022, doi: 10.1186/s41601-022-00238-x.

[3] Y. V. Hote and S. Jain, "PID controller design for load frequency control: Past, Present and future challenges," *IFAC-PapersOnLine*, vol. 51, no. 4, pp. 604–609, 2018, doi: 10.1016/j.ifacol.2018.06.162.

[4] N. K. Gupta, M. K. Kar, and A. K. Singh, "Design of a 2-DOF-PID controller using an improved sine–cosine algorithm for load frequency control of a three-area system with nonlinearities," *Protection Control Modern Power Syst.*, vol. 7, no. 1, pp. 1–18, Dec. 2022, doi: 10.1186/s41601-022-00255-w.

[5] G. Dei, D. K. Gupta, B. K. Sahu, A. V. Jha, B. Appasani, H. M. Zawbaa, and S. Kamel, "Improved squirrel search algorithm driven cascaded 2DOF-PID-FOI controller for load frequency control of renewable energy based hybrid power system," *IEEE Access*, vol. 10, pp. 46372–46391, 2022, doi: 10.1109/ACCESS.2022.3169749.

[6] L. Shen and H. Xiao, "Delay-dependent robust stability analysis of power systems with PID controller," *Chin. J. Electr. Eng.*, vol. 5, no. 2, pp. 79–86, Jun. 2019, doi: 10.23919/CJEE.2019.000014.

[7] J. Yang, Q. Zhong, K. Shi, Y. Yu, and S. Zhong, "Stability and stabilization for T–S fuzzy load frequency control power system with energy storage system," *IEEE Trans. Fuzzy Syst.*, vol. 32, no. 3, pp. 893–905, Mar. 2024, doi: 10.1109/TFUZZ.2023.3311925.

[8] C. J. Ramlal, A. Singh, S. Rocke, and M. Sutherland, "Decentralized fuzzy $H_\infty$-iterative learning LFC with time-varying communication delays and parametric uncertainties," *IEEE Trans. Power Syst.*, vol. 34, no. 6, pp. 4718–4727, Nov. 2019, doi: 10.1109/TPWRS.2019.2917613.

[9] A. H. Yakout, H. Kotb, H. M. Hasanien, and K. M. Aboras, "Optimal fuzzy PIDF load frequency controller for hybrid microgrid system using marine predator algorithm," *IEEE Access*, vol. 9, pp. 54220–54232, 2021, doi: 10.1109/ACCESS.2021.3070076.

[10] A. H. G. Haroun and Y.-Y. Li, "A novel optimized hybrid fuzzy logic intelligent PID controller for an interconnected multi-area power system with physical constraints and boiler dynamics," *ISA Trans.*, vol. 71, pp. 364–379, Nov. 2017.

[11] M. A. Kamarposhti, H. Shokouhandeh, M. Alipur, I. Colak, H. Zare, and K. Eguchi, "Optimal designing of fuzzy-PID controller in the load-frequency control loop of hydro-thermal power system connected to wind farm by HVDC lines," *IEEE Access*, vol. 10, pp. 63812–63822, 2022, doi: 10.1109/ACCESS.2022.3183155.

[12] M. Gheisarnejad and M. H. Khooban, "Design an optimal fuzzy fractional proportional integral derivative controller with derivative filter for load frequency control in power systems," *Trans. Inst. Meas. Control*, vol. 41, no. 9, pp. 2563–2581, Jun. 2019.

[13] M. Gheisarnejad, "An effective hybrid harmony search and cuckoo optimization algorithm based fuzzy PID controller for load frequency control," *Appl. Soft Comput.*, vol. 65, pp. 121–138, Jan. 2018.

[14] D. Tripathy, A. K. Barik, N. B. D. Choudhury, and B. K. Sahu, "Performance comparison of SMO-based fuzzy PID controller for load frequency control," in *Soft Computing for Problem Solving*. Singapore: Springer, 2019, pp. 879–892.

[15] A. Fathy, A. M. Kassem, and A. Y. Abdelaziz, "Optimal design of fuzzy PID controller for deregulated LFC of multi-area power system via mine blast algorithm," *Neural Comput. Appl.*, vol. 32, no. 9, pp. 4531–4551, May 2020.

[16] H. Y. Park and J. H. Kim, "The $l_1$ optimal state estimator for load frequency control of power systems: A comparative and extensive study," *IEEE Access*, vol. 10, pp. 120680–120689, 2022, doi: 10.1109/ACCESS.2022.3222487.

[17] A. G. Pillai, E. R. Samuel, and A. Unnikrishnan, "Optimal load frequency control through combined state and control gain estimation for noisy measurements," *Protection Control Modern Power Syst.*, vol. 5, no. 1, pp. 1–12, Dec. 2020, doi: 10.1186/s41601-020-00169-5.

[18] M. Jafari, M. A. Rahman, and S. Paudyal, "Optimal false data injection attack against load-frequency control in power systems," *IEEE Trans. Inf. Forensics Security*, vol. 18, pp. 5200–5212, 2023, doi: 10.1109/TIFS.2023.3305868.

[19] D. Guha, P. K. Roy, and S. Banerjee, "Multi-verse optimisation: A novel method for solution of load frequency control problem in power system," *IET Gener., Transmiss. Distrib.*, vol. 11, no. 14, pp. 3601–3611, Sep. 2017.

[20] N. Kouba, M. Menaa, K. Tehrani, and M. Boudour, "Optimal tuning for load frequency control using ant lion algorithm in multi-area interconnected power system," *Intell. Autom. Soft Comput.*, vol. 25, no. 2, pp. 279–294, 2019.

[21] J. Guo, "The load frequency control by adaptive high order sliding mode control strategy," *IEEE Access*, vol. 10, pp. 25392–25399, 2022, doi: 10.1109/ACCESS.2022.3152259.

[22] V. V. Huynh, P. T. Tran, C. S. T. Dong, B. D. Hoang, and O. Kaynak, "Sliding surface design for sliding mode load frequency control of multiarea multisource power system," *IEEE Trans. Ind. Informat.*, vol. 20, no. 5, pp. 7797–7809, May 2024, doi: 10.1109/TII.2024.3359445.

[23] S. Prasad, S. Purwar, and N. Kishor, "Non-linear sliding mode load frequency control in multi-area power system," *Control Eng. Pract.*, vol. 61, pp. 81–92, Apr. 2017.

[24] J. Guo, "Application of full order sliding mode control based on different areas power system with load frequency control," *ISA Trans.*, vol. 92, pp. 23–34, Sep. 2019.

[25] Q. Zhu and Z. Yang, "Intelligent power compensation system based on adaptive sliding mode control using soft computing and automation," *Comput. Syst. Sci. Eng.*, vol. 34, no. 4, pp. 179–189, 2019.

[26] J. Guo, "Application of a novel adaptive sliding mode control method to the load frequency control," *Eur. J. Control*, vol. 57, pp. 172–178, Jan. 2021.

[27] X. Lv, Y. Sun, Y. Wang, and V. Dinavahi, "Adaptive event-triggered load frequency control of multi-area power systems under networked environment via sliding mode control," *IEEE Access*, vol. 8, pp. 86585–86594, 2020.

[28] B. Le Ngoc Minh, V. V. Huynh, T. M. Nguyen, and Y. W. Tsai, "Decentralized adaptive double integral sliding mode controller for multi-area power systems," *Math. Problems Eng.*, vol. 2018, pp. 1–11, Oct. 2018.

[29] A. S. L. V. Tummala, R. Inapakurthi, and P. V. Ramanarao, "Observer based sliding mode frequency control for multi-machine power systems with high renewable energy," *J. Modern Power Syst. Clean Energy*, vol. 6, no. 3, pp. 473–481, May 2018.

[30] I. R. Fitri, J.-S. Kim, and H. Song, "High-gain disturbance observer-based robust load frequency control of power systems with multiple areas," *Energies*, vol. 10, no. 5, p. 595, Apr. 2017.

[31] S. Prasad, S. Purwar, and N. Kishor, "Load frequency regulation using observer based non-linear sliding mode control," *Int. J. Electr. Power Energy Syst.*, vol. 104, pp. 178–193, Jan. 2019.

[32] V. V. Huynh, B. L. N. Minh, E. N. Amaefule, A.-T. Tran, and P. T. Tran, "Highly robust observer sliding mode based frequency control for multi area power systems with renewable power plants," *Electronics*, vol. 10, no. 3, p. 274, Jan. 2021.

[33] V. V. Huynh, P. T. Tran, B. L. N. Minh, A. T. Tran, D. H. Tuan, T. M. Nguyen, and P.-T. Vu, "New second-order sliding mode control design for load frequency control of a power system," *Energies*, vol. 13, no. 24, p. 6509, Dec. 2020, doi: 10.3390/en13246509.

[34] M. K. Sarkar, A. Dev, P. Asthana, and D. Narzary, "Chattering free robust adaptive integral higher order sliding mode control for load frequency problems in multi-area power systems," *IET Control Theory Appl.*, vol. 12, no. 9, pp. 1216–1227, Jun. 2018.

[35] K. Liao and Y. Xu, "A robust load frequency control scheme for power systems based on second-order sliding mode and extended disturbance observer," *IEEE Trans. Ind. Informat.*, vol. 14, no. 7, pp. 3076–3086, Jul. 2018.

[36] V. Çelik, M. T. Özdemir, and K. Y. Lee, "Effects of fractional-order PI controller on delay margin in single-area delayed load frequency control systems," *J. Modern Power Syst. Clean Energy*, vol. 7, no. 2, pp. 380–389, Mar. 2019.

[37] R. Sepehrzad, A. Hedayatnia, M. Amohadi, J. Ghafourian, A. Al-Durra, and A. Anvari-Moghaddam, "Two-stage experimental intelligent dynamic energy management of microgrid in smart cities based on demand response programs and energy storage system participation," *Int. J. Electr. Power Energy Syst.*, vol. 155, Jan. 2024, Art. no. 109613, doi: 10.1016/j.ijepes.2023.109613.

[38] R. Sepehrzad, S. Nakhaeisharif, A. Al-Durra, M. Allahbakhshi, and A. Moridi, "Islanded micro-grid frequency control based on the optimal-intelligent Lyapunov algorithm considering power dynamic and communication uncertainties," *Electr. Power Syst. Res.*, vol. 208, Jul. 2022, Art. no. 107917, doi: 10.1016/j.epsr.2022.107917.

[39] R. Sepehrzad, A. Mahmoodi, S. Y. Ghalebi, A. R. Moridi, and A. R. Seifi, "Intelligent hierarchical energy and power management to control the voltage and frequency of micro-grids based on power uncertainties and communication latency," *Electr. Power Syst. Res.*, vol. 202, Jan. 2022, Art. no. 107567, doi: 10.1016/j.epsr.2021.107567.

[40] H. Shen, Y. Xia, J. Wang, and J. H. Park, "Fault-tolerant event-triggered $\mathcal{H}_\infty$ load frequency control for multiarea power systems with communication delay," *IEEE Syst. J.*, vol. 16, no. 4, pp. 6624–6634, Dec. 2022, doi: 10.1109/JSYST.2022.3149566.

[41] S. K. Pradhan and D. K. Das, "$H_\infty$ load frequency control design based on delay discretization approach for interconnected power systems with time delay," *J. Modern Power Syst. Clean Energy*, vol. 9, no. 6, pp. 1468–1477, Nov. 2021.

[42] S. Prasad, S. Purwar, and N. Kishor, "$H_\infty$ based non-linear sliding mode controller for frequency regulation in interconnected power systems with constant and time-varying delays," *IET Gener., Transmiss. Distrib.*, vol. 10, no. 11, pp. 2771–2784, Aug. 2016.

[43] Y. Sun, Y. Wang, Z. Wei, G. Sun, and X. Wu, "Robust $H_\infty$ load frequency control of multi-area power system with time delay: A sliding mode control approach," *IEEE/CAA J. Autom. Sinica*, vol. 5, no. 2, pp. 610–617, Mar. 2018.

[44] Y. Mi, X. Hao, Y. Liu, Y. Fu, C. Wang, P. Wang, and P. C. Loh, "Sliding mode load frequency control for multi-area time-delay power system with wind power integration," *IET Gener., Transmiss. Distrib.*, vol. 11, no. 18, pp. 4644–4653, Dec. 2017.

[45] A. E. Onyeka, Y. Xing-Gang, Z. Mao, B. Jiang, and Q. Zhang, "Robust decentralised load frequency control for interconnected time delay power systems using sliding mode techniques," *IET Control Theory Appl.*, vol. 14, no. 3, pp. 470–480, Feb. 2020.

[46] P. Chen, L. Yu, and D. Zhang, "Event-triggered sliding mode control of power systems with communication delay and sensor faults," *IEEE Trans. Circuits Syst. I, Reg. Papers*, vol. 68, no. 2, pp. 797–807, Feb. 2021, doi: 10.1109/TCSI.2020.3035603.

[47] F. Yang, Y. Shen, D. Li, S. Lin, S. M. Muyeen, H. Zhai, and J. Zhao, "Fractional-order sliding mode load frequency control and stability analysis for interconnected power systems with time-varying delay," *IEEE Trans. Power Syst.*, vol. 39, no. 1, pp. 1006–1018, Jan. 2024, doi: 10.1109/TPWRS.2023.3242938.

[48] S. Boyd, E. L. Ghaoui, E. Feron, and V. Balakrishna, *Linear Matrix Inequalities in System and Control Theory*. Philadelphia, PA, USA: Society For Industrial and Applied Mathematics, 1994.

**DAO HUY TUAN** received the master's degree in thermal engineering from Vietnam University of Technology, in 2013. He is currently pursuing the Ph.D. degree in electrical engineering with Ton Duc Thang University. His research interests include power systems and control systems.

**JAN PIDANIC** (Senior Member, IEEE) received the M.Sc. and Ph.D. degrees from the University of Pardubice, in 2005 and 2012, respectively. His research interests include signal processing in passive radar systems, bistatic radars, clutter modeling, and optimization of signal processing algorithms with parallel processing techniques.

**VAN VAN HUYNH** was born in Ho Chi Minh City, Vietnam. He received the Ph.D. degree in mechanical and automation control engineering from Da-Yeh University, Taiwan, in 2015. His current research interests include sliding mode control, variable structure control, and power system control.

**VO HOANG DUY** was born in Ho Chi Minh City, Vietnam. He received the Ph.D. degree in mechatronics from Pukyong National University, South Korea, in 2010. His research interests include robotics, automation, and industrial systems.

**NGUYEN HUU KHANH NHAN** received the Ph.D. degree from the Institute of Research and Experiments for Electrical and Electronic Equipment, Moscow, Russia. He is currently a Lecturer with the Faculty of Electrical and Electronic Engineering, Ton Duc Thang University, Ho Chi Minh City, Vietnam. His research interests include VLSI, MEMS, LED driver chips, robotics vision, robot navigation, and 3D video processing.